ACS SyntheticBiology

Letter

pubs.acs.org/synthbio

Optically Controlled Signal Amplification for DNA Computation

Alexander Prokup, James Hemphill, Qingyang Liu, and Alexander Deiters*

Department of Chemistry, University of Pittsburgh, Pittsburgh, Pennsylvania 15217, United States

Supporting Information

ABSTRACT: The hybridization chain reaction (HCR) and fuel−catalyst cycles have been applied to address the problem of signal amplification in DNA-based computation circuits. While they function efficiently, these signal amplifiers cannot be switched ON or OFF quickly and noninvasively. To overcome these limitations, a light-activated initiator strand for the HCR, which enabled fast optical OFF → ON switching, was developed. Similarly, when a light-activated version of the catalyst strand or the inhibitor strand of a fuel−catalyst cycle was applied, the cycle could be optically switched from OFF → ON or ON → OFF, respectively. To move the capabilities of these devices beyond solution-based operations, the components were embedded in agarose gels. Irradiation with customizable light patterns and at different time points demonstrated both spatial and temporal control. The addition of a translator gate enabled a spatially activated signal to travel along a predefined path, akin to a chemical wire. Overall, the addition of small light-cleavable photocaging groups to DNA signal amplification circuits enabled conditional control as well as fast photocontrol of signal amplification.

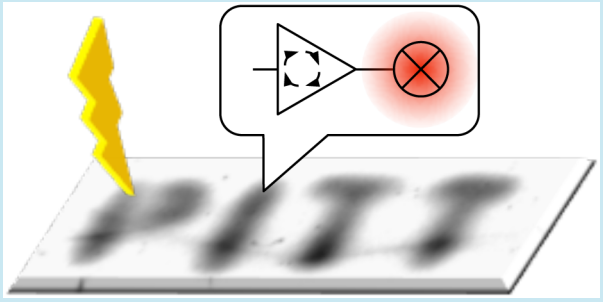

KEYWORDS: *DNA computation, signal amplification, photochemistry, hybridization chain reaction, fuel−catalyst cycle*

The field of DNA computation encompasses a wide variety of DNA-based devices, which attempt to utilize the strict control inherent to electronic circuits for biological problems. A variety of nucleic acid tools exist with unique functions,[1−3] for example, logic gate operation,[4−6] memory simulation,[7] game simulation,[8,9] protein translation activation,[10] and edge detection.[11] In order to operate, the devices require an exchange of DNA strands between logic gates, which can become inefficient in large circuits, leading to a dampening in signal.[5] Options are available to amplify a low DNA output signal: for example, the use of branched DNA to accumulate labeled DNA strands on an output strand,[12] a kinetically trapped metastable DNA fuel,[13] the hybridization chain reaction (HCR),[14,15] and an entropy-driven fuel−catalyst cycle.[16,17] However, the aforementioned amplification methods are limited in their ability to be externally controlled, particularly in a temporal and spatial fashion. Therefore, we developed light-regulated variants of HCR and fuel−catalyst cycle amplification for DNA computation. Our design relies on introducing nucleobase-caging groups into DNA strands[18−20] to sterically block DNA/DNA hybridization until irradiation with UV light induces caging group removal and DNA duplex formation.[21,22] Thus, a simple chemical modification to an existing structure enables the DNA amplification devices to be either turned ON or OFF through application of photochemical triggers in a spatial and temporal manner. Caging groups have already been applied to other DNA nanotechnology devices, such as antisense agents,[19] logic gates,[4,6] transcription factor decoys,[21] protein aptamers,[23,24] DNA minicircle assembly,[25] and deoxyribozymes.[26] Additionally, other DNA modifications have enabled strand ligation,[27] photocontrolled molecular beacons,[28] or reversible strand hybridization.[29] These examples show how light can be incorporated into DNA nanotechnology as a stimulus to initiate and control DNA hybridization cascades as well as genetic circuits.[11,30]

HCR allows for the detection of small concentrations of nucleic acids by generating an amplified signal through the opening of metastable hairpins to form a long nicked duplex, even in complex biological environments.[31] Three components are required for the reaction: two hairpins and an initiator strand. In the absence of the initiator, the hairpins will not cross react, as there are no complementary sequences exposed. However, when the initiator is added, it will hybridize to the toehold of hairpin 1 (H1) and expose a toehold for hairpin 2 (H2). After H2 binds to H1, a new toehold will be revealed, allowing the concatemer to continue growing. Overall, the presence of the input signal (i.e., the initiator strand) is amplified through the production of high molecular weight duplexes. To obtain optical control over HCR, the initiator strand was blocked with nucleobase caging groups to prevent binding to H1. Activation of the initiator strand is achieved by irradiation with UV light to photochemically remove the caging groups. Consequently, UV irradiation can act as a switch to turn on HCR (Figure 1a). Our design utilizes the known hairpin and initiator sequences published by the Pierce group,[14] with modified toehold regions to increase the number of thymidines. These hairpin sequences have been designed to prevent premature signal generation in the absence of initiator.

Received: July 19, 2014
Published: January 26, 2015

DOI: 10.1021/sb500279w
ACS Synth. Biol. 2015, 4, 1064−1069

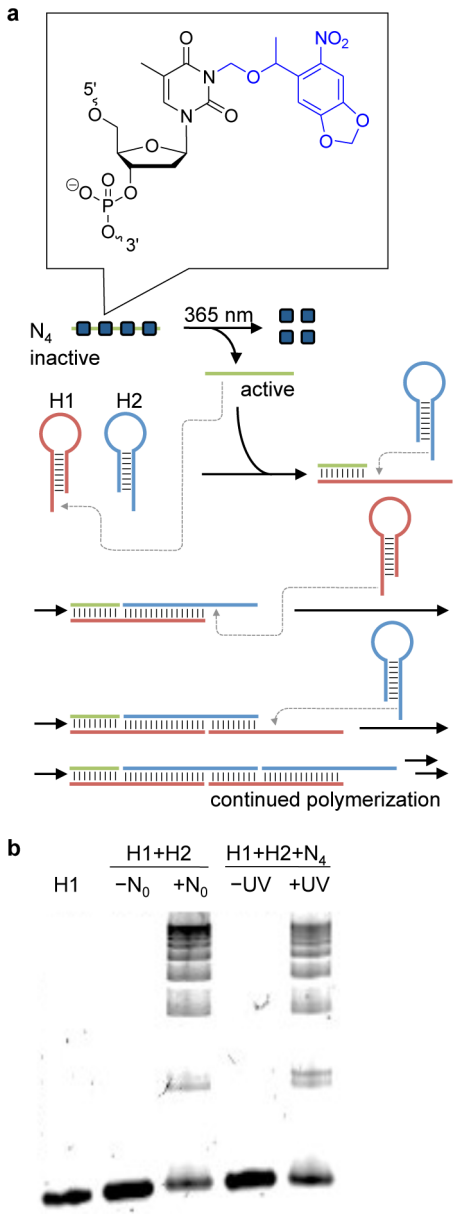

Figure 1. (a) Schematic of the hybridization chain reaction with the caged initiator strand N_4. Oligonucleotides are shown as colored lines, and caging groups are represented by blue boxes. Two hairpins (H1 and H2) are metastable until light-triggering of the initiator strand causes the formation of higher molecular weight product strands. (b) PAGE analysis of HCR reactions with noncaged (N_0) and caged initiator (N_4) strands. No background is observed in the absence of UV light. Irradiation of N_4 with UV light triggers the formation of higher molecular weight products similar to the HCR products produced by N_0.

The extra thymidine residues also allowed for increased flexibility in selecting nucleobases to cage.

Before optical control could be investigated, proper function of HCR needed to be ensured. Oligonucleotides were combined in solution, incubated overnight, and analyzed by gel electrophoresis. As expected, HCR only occurred when both hairpins and initiator strand were present (Figure 1b). To photochemically control HCR, four caging groups were added to the initiator, creating strand N_4. Four caging groups were selected based on previous experiments with caged oligomers, which demonstrated photochemical control of DNA/DNA hybridization with a nucleobase caging group every 4−5 bases.[22] In the absence of UV light, no HCR occurred and no higher molecular weight products were formed. Removal of the caging groups through UV exposure restored activity to the initiator, which was evident by the formation of the same HCR products as were produced by the noncaged initiator. Thus, photochemical control of HCR was achieved through a synthetic modification of a single DNA component.

Previously, HCR has been photochemically controlled with a cleavable backbone linker incorporated into a third hairpin structure.[32] When irradiated, the photolyzed hairpin would create initiator strands for HCR. However, applying a third hairpin as a blocked initiator strand caused a steady increase in background signal over the course of the reaction. After only 45 min, the background signal was nearly 20% of the highest obtained signal. This is in contrast to our results, which show no observable signs of product formation before decaging, even after an overnight reaction (Figure 1b and Supporting Information Figure 1) and thus show no background leakiness of the system. Additionally, full HCR activation is observed after only 90 s of irradiation (Supporting Information Figure 1) compared to 20 min in the case of the previous design.[32]

A second DNA-based device to achieve signal amplification involves a fuel−catalyst cycle.[16] The cycle begins with binding of the catalyst strand to the substrate complex (duplex containing the substrate, signal, and output strands). After a toehold mediated strand exchange, the catalyst displaces the signal strand revealing a toehold for the fuel strand. Binding of the fuel strand completely removes the output strand and catalyst, which creates a waste duplex. Displacement of the catalyst strand allows the cycle to continue, and the output strand is then able to interact with the reporter gate, releasing the quencher strand from the fluorophore strand. Thus, an increase in fluorescence corresponds to an active cycle. The fuel−catalyst cycle amplification arises from the release of a surplus of signal and output strands from a limited supply of catalyst. If the catalyst strand is caged (as in C_4), the caging groups will prevent activation of the cycle by blocking hybridization of the catalyst strand to the substrate complex. Removal of the caging groups with 365 nm light will create free catalyst strands thereby initiating the cycle (Figure 2a). To turn the amplification cycle OFF, an inhibitor strand I_4 was conceived, which is completely complementary to the catalyst thereby blocking its function. When the inhibitor strand is caged, hybridization to the catalyst is prevented and the cycle operates normally. After irradiation, the inhibitor will bind to the catalyst prohibiting continuation of the cycle. In order to generate a fluorescent output signal, a reporter gate can be added (Figure 2b and Supporting Information Figure 2a). The gate will interact with the output strand, releasing the fluorophore strand. The free fluorophore is then able to emit a fluorescent signal. Activation or deactivation of the cycle through photochemical means enables reliable regulation of amplification by precisely optically switching the cycle from either OFF → ON or ON → OFF.

Oligonucleotide strands and preformed gate structures were mixed in solution and assessed by gel electrophoresis (Supporting Information Figure 3) or fluorescence emission. After replacing C_0 with the caged C_4, no signal was produced, effectively turning the amplification cycle OFF (Figure 3a). Removal of the caging groups with UV light restored catalyst activity, generating a signal. Conversely, introduction of I_4 to the substrate complex, fuel strand, and C_0 did not affect normal

DOI: 10.1021/sb500279w
ACS Synth. Biol. 2015, 4, 1064−1069

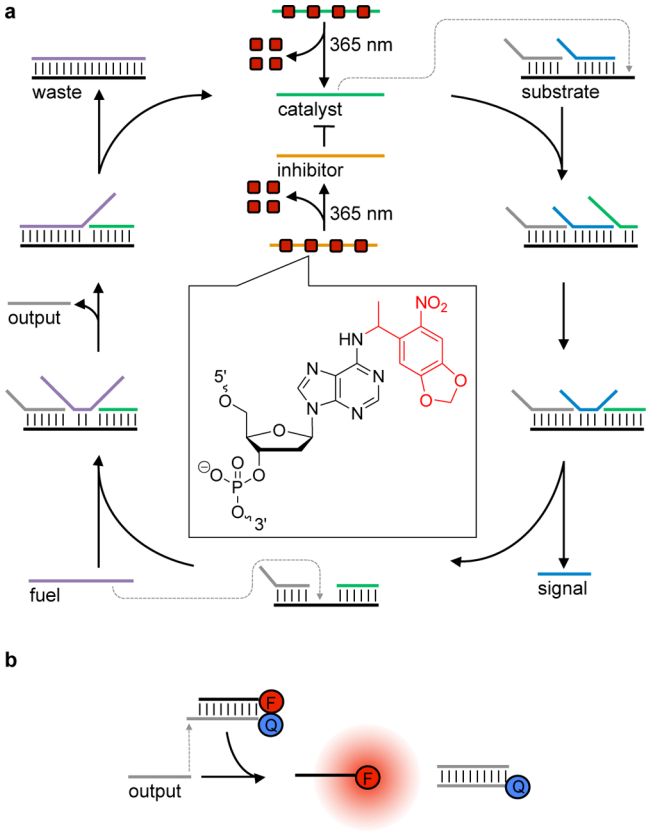

Figure 2. Schematic of the (a) fuel−catalyst cycle with caged inhibitor and caged catalyst strands and (b) fluorescence reporter gate. Colored lines represent DNA oligomers and red boxes indicate caging groups. In the absence of caging groups, adding a catalyst strand to the substrate complex and fuel strands will release the signal and output strands while creating a waste duplex. The output strand is able to interact with the reporter gate, releasing a fluorophore strand. F = TAMRA fluorophore, Q = BlackHole quencher-2.

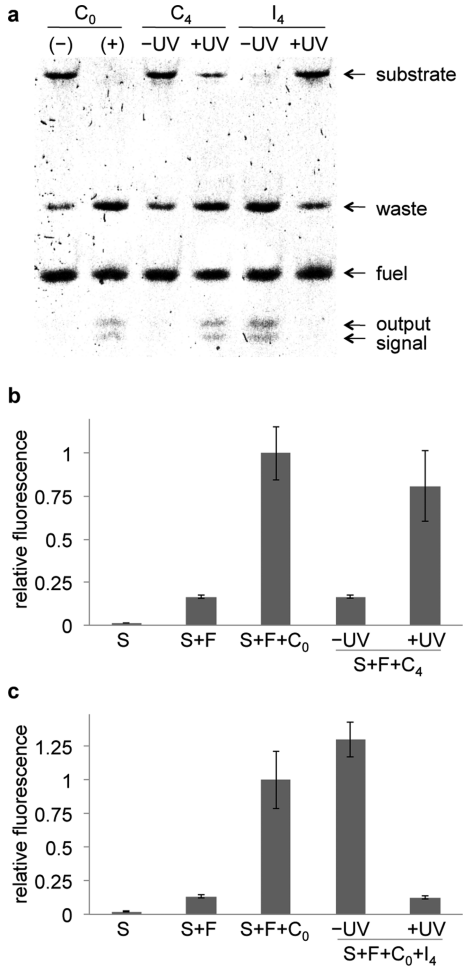

Figure 3. Optical OFF → ON and ON → OFF switching of the fuel−catalyst cycle by using caged catalyst and caged inhibitor strands. (a) Native-PAGE gel (16%) stained with SYBR Gold nucleic acid stain. Photochemical control is accomplished with the addition of caged catalyst (C_0) or caged inhibitor (I_4). Irradiation with UV light turns the fuel−catalyst cycle (without reporter gate) ON or OFF using the caged catalyst or caged inhibitor, respectively. Fluorescence quantification for the fuel−catalyst cycle after the addition of (b) C_4 or (c) I_4 using a reporter gate. Samples labeled +UV were irradiated with 365 nm light for 10 min before addition. Additional single letter abbreviations are used for substrate (S) and fuel (F). Excitation and emission wavelengths were 545 and 585 nm, respectively. Error bars represent standard deviations from three independent experiments.

operation of the cycle, and strand exchange cascades continued to produce signal. However, irradiating the caged inhibitor strand prevented amplification by sequestration of the catalyst strand, which switched the cycle OFF. Thus, the activity of the fuel−catalyst cycle could be photochemically controlled through the use of the caged inhibitor or caged catalyst strand. A fluorescence reporter gate was also used to measure the activity of the fuel−catalyst cycle, and confirmed the switching behavior of the caged oligonucleotides in the presence of UV irradiation (Figure 3b and c). More than 5-fold change in fluorescence signal was observed upon light-activation of the caged catalyst or caged inhibitor strand. This corresponds to efficient photoswitching of the amplification cycle, since a similar change was observed for the addition of noncaged catalyst and inhibitor strands. When fluorescence was measured over time for the fuel−catalyst cycle in the presence of the caged catalyst (Supporting Information Figure 4a), a steep increase in the fluorescence signal was observed only after irradiation with UV light. Addition of the caged inhibitor to the cycle did not affect normal output, whereas the decaged inhibitor strand blocked all signal production (Supporting Information Figure 4b).

With successful optical control of a solution-based amplification cycle, we next transitioned this system to semisolid media. Amplification of a signal inside a semisolid can expand the applications of DNA computation systems beyond solution-based devices, since it greatly constrains diffusion thereby enabling spatial control. Additionally, a solid structure creates a modular unit that could facilitate the physical separation of components in a DNA cascade. Much like electric components, embedded DNA computation devices can act as stand-alone elements of a larger circuit. To demonstrate spatial control of the fuel−catalyst cycle using the caged catalyst C_4, oligonucleotide components were embedded into low-melt agarose. Spatially restricted illumination of the gel with a fiber optics probe (Figure 4a and Supporting Information Movie 1) or through a mask (Figure 4b and Supporting Information Movie 2) enabled the amplification cycle to be activated in specific and independent regions. Although masks allowed for customizable shapes, the edges were not as well-defined as those produced by an LED fiber optic light source. To create a

DOI: 10.1021/sb500279w
ACS Synth. Biol. 2015, 4, 1064−1069

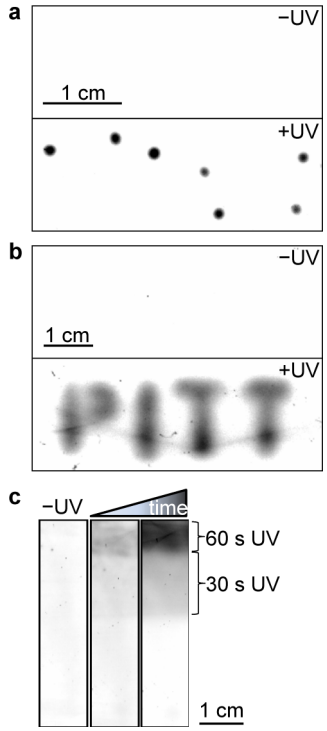

Figure 4. Spatial control of the fuel−catalyst cycle by using low-melt agarose gels (1−2%) embedded with the substrate complex, fuel strand, and caged catalyst C_4. (a) A fiber optics probe was used to irradiate (1 min, 365 nm) spatially independent areas in the shape of the big dipper constellation. (b) Illumination through a mask was used to pattern "PITT". (c) Multiple irradiation time intervals were used to create a gradient effect, tuning activation of the catalyst cycle. All fluorescent imaging was performed using green LED excitation, and emitted light was detected at 580−630 nm.

gradient effect, the gel was irradiated for different time intervals (Figure 4c). The gradient demonstrated how signal intensity could be tuned by varying the applied UV irradiation. Variable light intensities will create diverse populations of signal intensity, adding depth to the recognition of an OFF → ON transition. The ability to create signals in any desired pattern using optical regulation could allow for better control in investigating or modeling biological events. In addition to patterning, the system can be engineered to allow for signal propagation from a defined start point through a gel. A translator gate was added to the fuel−catalyst system to produce a second catalyst strand from the signal strand (Supporting Information Figure 5). When the cycle is triggered through light exposure, the signal propagates from the point of irradiation. Unlike the cycle without the translator gate, which expands minimally after an hour through simple diffusion of the decaged catalyst (Supporting Information Figure 6), the signal strand can activate new catalyst cycles in neighboring regions by interacting with the new translator gate, thereby counteracting dilution of the catalyst and instead facilitating signal propagation. In regions where the signal strand is not available yet, the translator gate will remain hybridized as a duplex and will not be able to release additional catalyst. When the translator gate is added but the circuit is not irradiated, the signal only increases minimally. Thus, localized UV irradiation generates a signal that continues to travel in the shape of the gel. Movement of the signal along a specific, predefined path is analogous to a chemical wire. Similar to electrical circuits, this may allow for the communication of spatially separated DNA computation devices with each other. Activation of spatially defined areas at multiple time intervals demonstrated spatiotemporal activation of the fuel−catalyst cycle (Supporting Information Figure 7 and Movie 3). Three separate signals appear relatively quickly after irradiation with a fiber optics probe. Temporal control is advantageous in order to tune the cycle to external events. A signal output is no longer restricted to a single location or pattern and can be changed manually to desired specifications with minimal irradiation. Thus, spatial and temporal control of the gel-based fuel−catalyst cycle offers enhanced flexibility in controlling signal amplification.

In conclusion, modification of oligonucleotides with nucleobase-caging groups enabled optical control over HCR and a fuel−catalyst cycle, DNA devices that allow for a DNA signal amplification. Crucial DNA strands were modified with photocleavable caging groups to optically control the individual reaction circuits. For HCR, a caged initiator strand was synthesized. Upon decaging, the initiator strand was able to interact with the hairpins, causing amplification through DNA strand polymerization. Only a low concentration of initiator is necessary to start the HCR, which can be achieved through minimal light exposure. A fuel−catalyst cycle was also successfully optically switched from OFF → ON or ON → OFF by using either a caged catalyst or a caged inhibitor, respectively. To prevent DNA/DNA hybridization in the absence of illumination, and thus to control the cycle with light, four evenly spaced caging groups were added to the DNA strands. Quantification of the output was made possible with a reporter gate generating a fluorescent signal. Conducting light-activation in a semisolid containing the DNA circuits led to remarkable spatial and temporal control. Localized illumination of the gel embedded with the DNA circuits enabled triggering of signal amplification in customizable patterns as well as tunable gradients. Furthermore, the fuel−catalyst cycle was modified with an additional translator gate and converted into a light-triggered autocatalytic cycle that enabled directional signal propagation in a preshaped agarose gel. In addition to spatial activation, the amplification cycle was also temporally activated. For each cycle, light acts as a dependable switch for triggering computational events as it is tunable and noninvasive. Caged oligonucleotides represent a modular framework that can be easily fitted to existing DNA-based architectures.

The methodology development reported here may find application in more complex DNA computation circuits that contain an output amplification. Temporal control enables precise sequencing of gate and subnetwork functions and, in the case of temporal control of an amplification cycle, allows for upstream circuit completion before output amplification, thereby potentially reducing the background signal by preventing premature activation. In addition, temporal control of DNA circuits enables modification of any system (e.g., drug treatment of cells) that is interfaced with a DNA computation network before circuit activation. Light is an excellent external control element that can be used as a switch with very high temporal and spatial resolution without the need for other physical or chemical alterations (e.g., injections). The application of light-activated DNA circuits and amplification devices is especially advantageous in systems that do not allow for later addition of oligonucleotide triggers, for example, in semisolid media as shown here or in enclosed biological environments, such as organisms.

DOI: 10.1021/sb500279w
ACS Synth. Biol. 2015, 4, 1064−1069

METHODS

Oligonucleotide Synthesis. DNA synthesis was performed using an Applied Biosystems (Foster City, CA) model 394 automated DNA/RNA synthesizer and standard β-cyanoethyl phosphoramidite chemistry. The caged oligonucleotides were synthesized on a 40 nmol scale, with solid-phase supports obtained from Glen Research (Sterling, VA). Reagents for automated DNA synthesis were also obtained from Glen Research. Standard synthesis cycles provided by Applied Biosystems were used for all normal bases with 25 s coupling times. The coupling time was increased to 2 min for incorporation of caged deoxythymidine modified phosphoramidite. The NPOM-caged deoxythymidine phosphoramidite was resuspended in anhydrous acetonitrile to a concentration of 0.1 M. Unmodified oligonucleotides were purchased from Integrated DNA Technologies (IDT).

HCR with Caged Initiator. Hairpins H1 (3 μM) and H2 (3 μM) were annealed (95 to 4 °C) independently in HCR buffer (50 mM Na_2HPO_4, 0.5 M NaCl, pH 6.8) prior to testing. Hairpins H1 and H2 (used at a final concentration of 1 μM) were combined with initiator strand (used at a final concentration of 0.33 μM) and allowed to react (overnight, room temperature). Reactions were analyzed by native-PAGE (16%, 100 V, 1 h), stained (SYBR Gold nucleic acid stain), and imaged (General Electric Typhoon FLA 7000 phosphorimager).

Assembly of Substrate Complex, Reporter Gate, and Translator Gate. Oligonucleotides S_{base}, S_{output}, and S_{signal} (Supporting Information Table 1) were combined (60 μM each component) with TE/Mg^{2+} buffer (10 mM Tris, 1 mM EDTA, 12.5 mM $MgCl_2$, pH 8) and annealed slowly (95 to 4 °C). The solution was then run on a 16% native-PAGE gel (100 V, 1 h). Bands were illuminated on a TLC plate with a hand-held UV light and excised with a razor blade. The substrate complex was eluted (using TE/Mg^{2+} buffer) from the gel on a shaker (room temperature, overnight) and quantified using nearest-neighbor models. The reporter gate (RG) was made using the same procedure, but with the R_F and R_Q oligonucleotides; similarly, the translator gate used the oligonucleotides T_{base} and T_{output}.

Fuel−Catalyst Cycle with Caged Oligonucleotides Gel Analysis. A reaction mixture (20 μL) was made in TE/Mg^{2+} buffer with the substrate complex (S, 200 nM), fuel strand (F, 200 nM), and catalyst (C, 20 nM, Supporting Information Table 1). When appropriate, the caged catalyst strand (C_4, 20 nM), inhibitor (I, 100 nM) or caged inhibitor strand (I_4, 100 nM) was added and decaged (365 nm light, 10 min). After the fuel−catalyst cycle was completed (room temperature, overnight), the reactions were loaded onto a 16% native-PAGE gel (100 V, 1 h), stained (SYBR Gold nucleic acid stain), and imaged (General Electric Typhoon FLA 7000 phosphorimager).

Fluorescence Quantification. In a black walled 96-well plate, reactions were set up in TE/Mg^{2+} buffer containing the substrate complex (S, 800 nM), reporter gate (RG, 200 nM), and fuel strand (F, 850 nM, Supporting Information Table 1). Where necessary, the catalyst (C, 80 nM), caged catalyst (C_4, 200 nM), inhibitor (I, 240 nM), or caged inhibitor strand (I_4, 240 nM) was added and decaged (365 nm light, 10 min). The fuel−catalyst cycle was allowed to react (room temperature, 3 h) and quantified by a plate reader (excitation/emission 545/585 nm, Tecan Infinite M1000 Pro). Fluorescence measurements were recorded every 15 min (room temperature) in a black walled 96-well plate, with substrate complex (S, 800 nM), reporter gate (RG, 200 nM), fuel strand (F, 850 nM), and caged catalyst (C_4, 20 nM) or caged inhibitor (I_4, 240 nM). The caged inhibitor was irradiated (365 nm, 10 min) before measuring fluorescence, whereas the caged catalyst was irradiated after recording fluorescence for 30 min.

Fuel−Catalyst Spatial Control. Spatial control was performed in low-melt agarose gel (1−2%) prepared with TE/Mg^{2+} buffer and solidified on a glass microscope slide. Before solidification, the substrate complex (S, 200 nM), fuel strand (F, 200 nM), reporter gate (RG, 50−200 nM), caged catalyst (C_4, 50 nM), and if necessary, translator gate (TG, 20 nM) were added together (500 μL). This solution was mixed with a 2× concentrated low-melt agarose solution (500 μL) so that the final gel percentage was 1−2% in a 1 mL total volume solution. Agarose solution was also allowed to cool to almost room temperature before mixing to prevent denaturating the preformed DNA/DNA duplexes. The gel was irradiated with UV light (0.5−1 min) through a patterned foil mask on a transilluminator (UVP high performance UV transilluminator) or with a UV fiber optics probe (1−5 min). The gel was then imaged for fluorescence (green excitation LEDs, 605/50 filter, ChemiDoc MP Imaging System).

Concentrations for experiments shown in Figure 4 and Supporting Information Figure 7: 200 nM substrate complex, 200 nM fuel, 50 nM reporter gate, and 50 nM caged catalyst. Concentrations for experiments shown in Supporting Information Figure 6: 200 nM substrate complex, 200 nM fuel, 200 nM reporter gate, 50 nM caged catalyst, and 20 nM translator gate.

ASSOCIATED CONTENT

Supporting Information

Supporting Figures 1−7: Native-PAGE gels; fuel-catalyst cycle schematics; time-course fluorescent measurements for the fuel−catalyst cycle; spatio-temporal control of the fuel−catalyst cycle in a semi-solid. Supporting movies. Supporting Table 1: Sequences of oligonucleotides. This material is available free of charge via the Internet at http://pubs.acs.org.

AUTHOR INFORMATION

Corresponding Author

*E-mail: deiters@pitt.edu. Tel: 412-624-5515.

Notes

The authors declare no competing financial interest.

REFERENCES

(1) Chen, X., and Ellington, A. D. (2010) Shaping up nucleic acid computation. *Curr. Opin. Biotechnol. 21*, 392−400.

(2) Jung, C., and Ellington, A. D. (2014) Diagnostic applications of nucleic acid circuits. *Acc. Chem. Res. 47*, 1825−1835.

(3) Krishnan, Y., and Simmel, F. C. (2011) Nucleic acid based molecular devices. *Angew. Chem., Int. Ed. Engl. 50*, 3124−3156.

(4) Prokup, A., Hemphill, J., and Deiters, A. (2012) DNA computation: A photochemically controlled AND gate. *J. Am. Chem. Soc. 134*, 3810−3815.

(5) Seelig, G., Soloveichik, D., Zhang, D. Y., and Winfree, E. (2006) Enzyme-free nucleic acid logic circuits. *Science 314*, 1585−1588.

(6) Hemphill, J., and Deiters, A. (2013) DNA computation in mammalian cells: microRNA Logic Operations. *J. Am. Chem. Soc. 135*, 10512−10518.

(7) Qian, L., Winfree, E., and Bruck, J. (2011) Neural network computation with DNA strand displacement cascades. *Nature 475*, 368−372.

DOI: 10.1021/sb500279w
ACS Synth. Biol. 2015, 4, 1064−1069

(8) Stojanovic, M. N., and Stefanovic, D. (2003) A deoxyribozyme-based molecular automaton. *Nat. Biotechnol. 21*, 1069−1074.
(9) Macdonald, J., Li, Y., Sutovic, M., Lederman, H., Pendri, K., Lu, W., Andrews, B. L., Stefanovic, D., and Stojanovic, M. N. (2006) Medium scale integration of molecular logic gates in an automaton. *Nano Lett. 6*, 2598−2603.
(10) Anderson, J. C., Voigt, C. A., and Arkin, A. P. (2007) Environmental signal integration by a modular AND gate. *Mol. Syst. Biol. 3*, 133.
(11) Tabor, J. J., Salis, H. M., Simpson, Z. B., Chevalier, A. A., Levskaya, A., Marcotte, E. M., Voigt, C. A., and Ellington, A. D. (2009) A synthetic genetic edge detection program. *Cell 137*, 1272−1281.
(12) Collins, M. L., Irvine, B., Tyner, D., Fine, E., Zayati, C., Chang, C., Horn, T., Ahle, D., Detmer, J., Shen, L. P., Kolberg, J., Bushnell, S., Urdea, M. S., and Ho, D. D. (1997) A branched DNA signal amplification assay for quantification of nucleic acid targets below 100 molecules/mL. *Nucleic Acids Res. 25*, 2979−2984.
(13) Seelig, G., Yurke, B., and Winfree, E. (2006) Catalyzed relaxation of a metastable DNA fuel. *J. Am. Chem. Soc. 128*, 12211−2220.
(14) Dirks, R. M., and Pierce, N. A. (2004) Triggered amplification by hybridization chain reaction. *Proc. Natl. Acad. Sci. U.S.A. 101*, 15275−15278.
(15) Choi, H. M., Beck, V. A., and Pierce, N. A. (2014) Next-generation *in situ* hybridization chain reaction: Higher gain, lower cost, greater durability. *ACS Nano 8*, 4284−4294.
(16) Zhang, D. Y., Turberfield, A. J., Yurke, B., and Winfree, E. (2007) Engineering entropy-driven reactions and networks catalyzed by DNA. *Science 318*, 1121−1125.
(17) Zhang, D. Y., and Winfree, E. (2008) Dynamic allosteric control of noncovalent DNA catalysis reactions. *J. Am. Chem. Soc. 130*, 13921−13926.
(18) Deiters, A., Garner, R. A., Lusic, H., Govan, J. M., Dush, M., Nascone-Yoder, N. M., and Yoder, J. A. (2010) Photocaged morpholino oligomers for the light-regulation of gene function in zebrafish and *Xenopus* embryos. *J. Am. Chem. Soc. 132*, 15644−15650.
(19) Young, D. D., Lusic, H., Lively, M. O., Yoder, J. A., and Deiters, A. (2008) Gene silencing in mammalian cells with light-activated antisense agents. *ChemBioChem 9*, 2937−2940.
(20) Young, D. D., Lively, M. O., and Deiters, A. (2007) Activation and deactivation of DNAzyme and antisense function with light for the photochemical regulation of gene expression in mammalian cells. *J. Am. Chem. Soc. 132*, 6183−6193.
(21) Govan, J. M., Lively, M. O., and Deiters, A. (2011) Photochemical control of DNA decoy function enables precise regulation of nuclear factor κB activity. *J. Am. Chem. Soc. 133*, 13176−13182.
(22) Young, D. D., Edwards, W. F., Lusic, H., Lively, M. O., and Deiters, A. (2008) Light-triggered polymerase chain reaction. *Chem. Commun. (Camb.)*, 462−464.
(23) Pinto, A., Lennarz, S., Rodrigues-Correia, A., Heckel, A., O'Sullivan, C. K., and Mayer, G. (2012) Functional detection of proteins by caged aptamers. *ACS Chem. Biol. 7*, 360−366.
(24) Heckel, A., and Mayer, G. (2005) Light regulation of aptamer activity: An anti-thrombin aptamer with caged thymidine nucleobases. *J. Am. Chem. Soc. 127*, 822−823.
(25) Schmidt, T. L., Koeppel, M. B., Thevarpadam, J., Goncalves, D. P., and Heckel, A. (2011) A light trigger for DNA nanotechnology. *Small 7*, 2163−2167.
(26) Lusic, H., Lively, M. O., and Deiters, A. (2008) Light-activated deoxyguanosine: Photochemical regulation of peroxidase activity. *Mol. Biosyst. 4*, 508−511.
(27) Gerrard, S. R., Hardiman, C., Shelbourne, M., Nandhakumar, I., Norden, B., and Brown, T. (2012) A new modular approach to nanoassembly: Stable and addressable DNA nanoconstructs via orthogonal click chemistries. *ACS Nano 6*, 9221−9228.
(28) Qiu, L., Wu, C., You, M., Han, D., Chen, T., Zhu, G., Jiang, J., Yu, R., and Tan, W. (2013) A targeted, self-delivered, and photocontrolled molecular beacon for mRNA detection in living cells. *J. Am. Chem. Soc. 135*, 12952−12955.
(29) Nishioka, H., Liang, X., Kato, T., and Asanuma, H. (2012) A photon-fueled DNA nanodevice that contains two different photoswitches. *Angew. Chem., Int. Ed. Engl. 51*, 1165−1168.
(30) Gardner, L., and Deiters, A. (2012) Light-controlled synthetic gene circuits. *Curr. Opin. Chem. Biol. 16*, 292−299.
(31) Choi, H. M., Chang, J. Y., Trinh, l. A., Padilla, J. E., Fraser, S. E., and Pierce, N. A. (2010) Programmable *in situ* amplification for multiplexed imaging of mRNA expression. *Nat. Biotechnol. 28*, 1208−1212.
(32) Huang, F., You, M., Han, D., Xiong, X., Liang, H., and Tan, W. (2013) DNA branch migration reactions through photocontrollable toehold formation. *J. Am. Chem. Soc. 135*, 7967−7973.

DOI: 10.1021/sb500279w
ACS Synth. Biol. 2015, 4, 1064−1069